

A transparent epoxy vitrimer with outstanding flame retardancy, toughness, and recyclability enabled by a hyperbranched P/N-derived polyester

Guofeng Ye^a, Siqi Huo^{b,*}, Cheng Wang^a, Yong Guo^b, Qingshan Yang^b, Pingan Song^c, Hao Wang^b, Zhitian Liu^{a,*}

^a Hubei Engineering Technology Research Centre of Optoelectronic and New Energy Materials, School of Materials Science & Engineering, Wuhan Institute of Technology, Wuhan 430205, China

^b School of Engineering, Centre for Future Materials, University of Southern Queensland, Springfield 4300, Australia

^c School of Agriculture and Environmental Science, Centre for Future Materials, University of Southern Queensland, Springfield 4300, Australia

ARTICLE INFO

Keywords:

Flame retardancy
Recyclability
Vitrimer

ABSTRACT

Despite the tremendous advances in vitrimers, it is still a challenge to realize advanced vitrimers with high transparency, toughness, and fire safety. To achieve this performance portfolio, the closed-loop recyclable transesterification vitrimer (HPN_{1.80}) with excellent transparency, toughness, and flame retardancy was prepared by incorporating a hydroxy-terminated hyperbranched polyester (HPN) into diglycidyl ether of bisphenol-A (DGEBA)/methyl tetrahydrophthalic anhydride (MeTHPA) system. HPN was easily obtained by esterification of triethanolamine (TEOA) and 9,10-dihydro-10-(2,3-dicarboxypropyl)-9-oxa-10-phosphaphenanthrene 10-oxide (DDP). Owing to the favorable compatibility of HPN with the matrix, the resulting HPN_{1.80} exhibited a high transmittance of 85.9% at 700 nm, a toughness of 2.3 MJ/m³, and an impact strength of 4.5 kJ/m². The phosphorus-containing groups of HPN played an important role in the gas/condensed flame retardancy, allowing HPN_{1.80} to pass the vertical burning (UL-94) V-0 classification with a limiting oxygen index (LOI) of 32.6%. Due to the catalysis by hydroxyl and tertiary amines, the broken HPN_{1.80} can be recycled by hot-pressing at 200 °C for 1 h. The regenerated HPN_{1.80} achieved an LOI of 31.8% and a UL-94 V-0 rating even after two physical reprocessing cycles. For the carbon fiber-reinforced HPN_{1.80} (CF/HPN_{1.80}) composites, the non-destructive recycling of carbon fibers (CFs) can be achieved due to the presence of a degradable ester group within HPN_{1.80}. This work offers a rational strategy for creating advanced epoxy vitrimers with recyclability, transparency, toughening, and flame retardancy.

1. Introduction

Epoxy resin (EP), being a significant polymeric substance, is extensively utilized as the adhesive or matrix in composite materials for construction, transportation, and electrical appliances because of its excellent adhesive, solvent resistance, and electrical insulation properties [1,2]. Although the covalently crosslinked network gives EP great chemical resistance and stability, their recycling has become essential due to the growing demand for carbon fiber-reinforced polymer (CFRP) composites [3,4].

Introducing dynamic covalent networks (DCNs) is a proven approach to manufacture recyclable thermosets and CFRP composites [5–7].

Dynamic covalent polymers relying on an associative mechanism are named as vitrimers. The vitrimers can dynamically respond to external stimuli (e.g., light and heat) to achieve reprocessing, but maintain a constant cross-link density during the process [8,9]. Leibler et al. remodeled thermosetting resins at 240 °C by introducing 10 mol% zinc acetate into the epoxy/anhydride system [10]. However, it is difficult to disperse the catalyst uniformly at high loading, which reduces the mechanical properties of the resin, and the catalyst may leach out during long-term service, causing environmental and human health hazards. Therefore, it is essential to develop self-catalyzed vitrimers with greater application potential. Previous works have shown that introducing hydroxyl groups, carboxyl groups, tertiary amines, and α -CF₃, etc. into the

* Corresponding authors.

E-mail addresses: sqhuo@hotmail.com, Siqi.Huo@unisq.edu.au (S. Huo), able.ztliu@wit.edu.cn (Z. Liu).

<https://doi.org/10.1016/j.conbuildmat.2025.140673>

Received 3 December 2024; Received in revised form 20 February 2025; Accepted 1 March 2025

Available online 6 March 2025

0950-0618/© 2025 The Author(s). Published by Elsevier Ltd. This is an open access article under the CC BY license (<http://creativecommons.org/licenses/by/4.0/>).

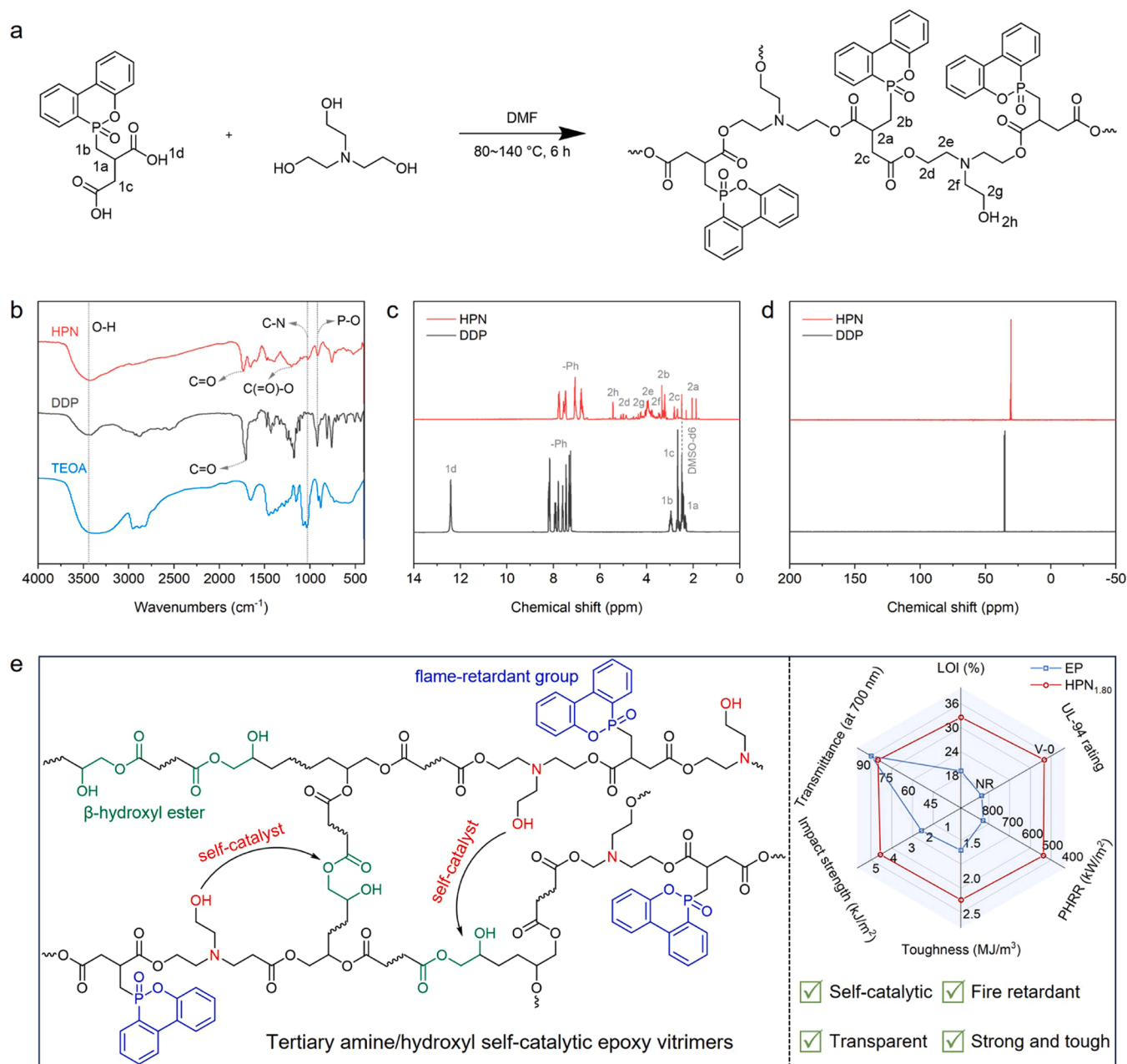


Fig. 1. (a) Synthetic route of HPN; (b) FTIR spectra of TEOA, DDP, and HPN; (c) ¹H NMR spectra and (d) ³¹P NMR spectra of DDP and HPN; and (e) schematic diagram of the transesterification mechanism in HPN_x vitrimer and comparison of the comprehensive performance for EP and HPN_{1.80}.

dynamic covalent network could achieve self-catalytic vitrimer [11–14]. For example, Yue et al. observed a significant relaxation process at 220 °C by introducing hydroxyl-rich cellulose nanocrystals (CNC) into an epoxy/anhydride system [15]. In particular, the abundant hydroxyl groups in the CNC not only catalyzed the transesterification, but were also covalently bonded to the matrix, allowing the CNC to be uniformly dispersed in the matrix.

Furthermore, the flammability of EPs is a major impediment to their high-tech applications [16,17]. Chen *et al.* incorporated phosphate ester and hydroxyl groups into the epoxy/anhydride system as flame-retardant and internal catalytic groups, respectively [18]. These groups allowed the resulting epoxy vitrimer to pass a UL-94 V-0 rating with an LOI of 37.3%, with the ability to be remolded at 180 °C. However, these vitrimers are typically characterized by undesirable mechanical properties, limiting their industrial applications. Therefore, developing high-tech vitrimers with favorable mechanical properties,

flame retardancy, and availability for preparing recyclable CFRP composites remains a great challenge.

In our previous works, it had been demonstrated that the hyperbranched polymers were capable of toughening and strengthening epoxy resins [19–21]. To solve the above difficulties, we synthesized a phosphorus/nitrogen/hydroxyl-rich hyperbranched polyester by a simple esterification reaction of DDP and TEOA, which was introduced into the EP/anhydride system to prepare a transparent, toughened, and flame-retardant self-catalytic vitrimer (HPN_{1.80}). HPN_{1.80} can be applied as a matrix for the manufacture of advanced CFRP composites, where both matrix and CFs can be chemically recycled due to the simultaneous introduction of tertiary amine and hydroxyl groups into the DCNs. As a result, this work offers a simple and implementable method to fabricate high-tech epoxy vitrimers.

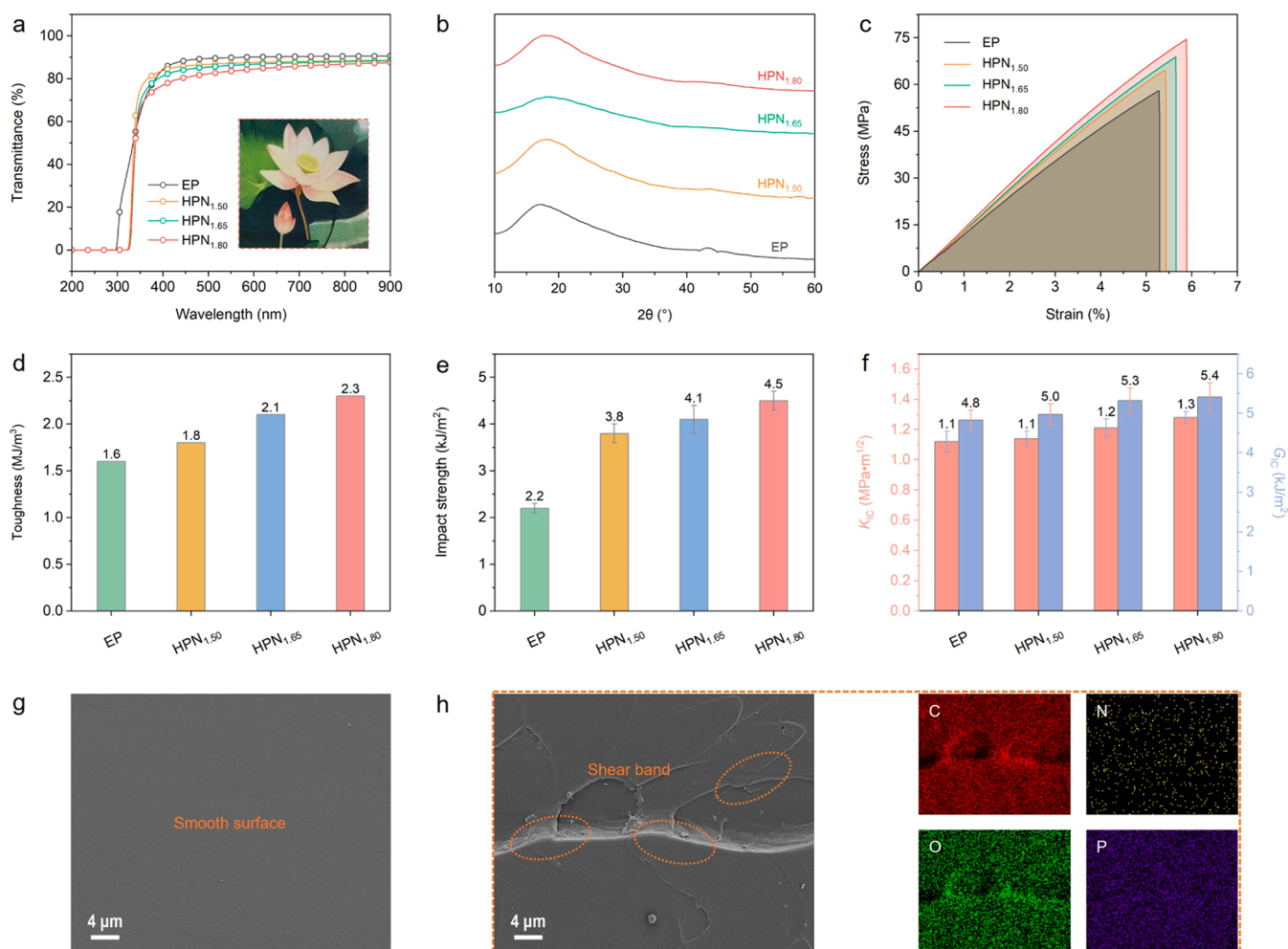


Fig. 2. (a) UV–visible transmission spectra of EP and HPN_x and the digital image of HPN_{1.80} film with the lotus as background (film size: 50 mm × 50 mm × 0.2 mm); (b) XRD patterns, (c) tensile stress–strain curves, (d) toughness, (e) impact strength and (f) K_{IC} and G_{IC} of EP and HPN_x, (g) SEM images of fractured surfaces for EP; and (h) SEM image and elemental mappings of fractured surface for HPN_{1.80}.

2. Materials and methods

2.1. Materials

The diglycidyl ether of bisphenol-A (DGEBA, E51) was purchased from Yueyang Baling Petrochemical Co, Ltd (Hunan, China). Methyl tetrahydrophthalic anhydride (MeTHPA), triethanolamine (TEOA), 2,4,6-tris(dimethylaminomethyl)phenol (DMP-30), tetrahydrofuran (THF), and *N,N*-dimethylformamide (DMF) were obtained from Macklin Biochemical Technology Co., Ltd. (Shanghai, China). 9,10-Dihydro-10-(2,3-dicarboxypropyl)-9-oxa-10-phosphaphenanthrene 10-oxide (DDP) was provided by Jianchu Biomedical Co., Ltd. (Hubei, China).

2.2. Synthesis of phosphorus/trialkylamine-containing hyperbranched polyester (HPN)

The synthesis routine of HPN is illustrated in Fig. 1a. HPN was easily obtained by esterification of TEOA and DDP. Briefly, DDP (10.0 g), TEOA (12.1 g), and DMF (100 mL) were added to a single-necked flask equipped with a condenser and water divider. The mixture was stirred at 80, 120, and 140 °C for 2 h, respectively. Finally, HPN (a yellowish powder) was gathered through rotary evaporation and drying in an oven (Yield: 98.2%).

2.3. Preparation of HPN-containing vitrimer (HPN_x) and CF/HPN_{1.80}

The specific formulations of HPN_x vitrimers are presented in Table S1, and x indicates the phosphorus content of the vitrimer. Taking HPN_{1.50} as an example, HPN (21.0 g) and DGEBA (42.8 g) were positioned in a flask, and they were mixed at 120 °C for 1 h until a transparent solution was obtained. After cooling to 75 °C, MeTHPA (36.2 g) was introduced to the flask, and the resulting liquids were stirred for 12 min. After eliminating the foam for 3 min, the mixture was placed in a stainless steel mold, and cured at 120 and 150 °C for 4 h, respectively. EP was manufactured in the same manner but replacing HPN with DMP-30.

The CF/HPN_{1.80} composites (CF: HPN_{1.80} = 6: 4, w/w) were fabricated by combining hand lay-up and hot-pressing. First, the CFs were placed on a stainless-steel plate and saturated with the uncured HPN_{1.80} mixture by hand lay-up. The above steps were repeated six times, and the prepreg with six layers of CFs was obtained. Finally, the CF/HPN_{1.80} composite was acquired by means of hot pressing at 160 °C for 2 h and under a pressure of 5 MPa.

2.4. Characterizations

This section is presented in the Supporting Information.

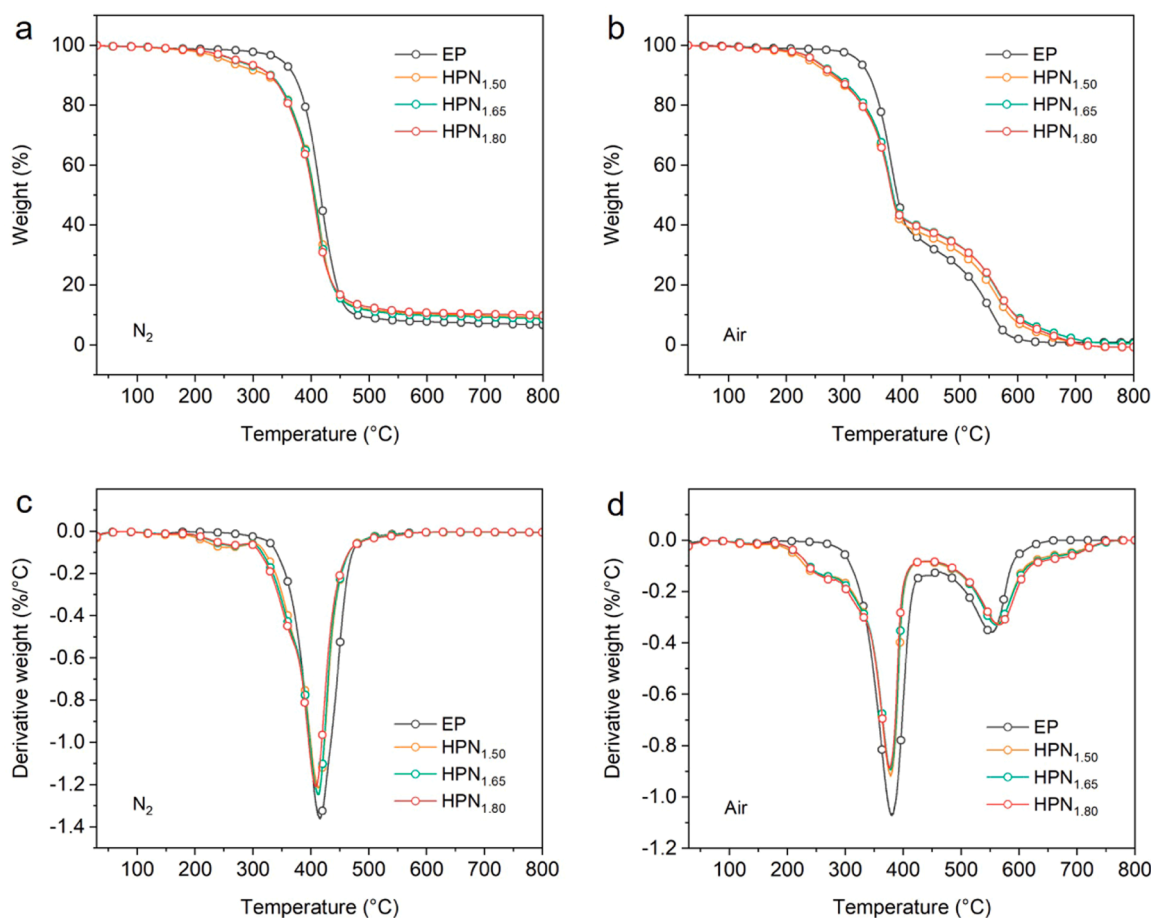


Fig. 3. (a) TG and (c) derivative TG (DTG) curves of EP and HPN_x in N₂ condition; and (b) TG and (d) DTG curves of EP and HPN_x under airflow.

3. Results and discussion

3.1. Characterization of HPN

The chemical structure of HPN was identified by using Fourier transform infrared (FTIR), nuclear magnetic resonance (NMR), and gel permeation chromatography (GPC), and the corresponding results are demonstrated in Figs. 1b-d and S1. The FTIR spectra of TEOA, DDP, and HPN are presented in Fig. 1b. Regarding TEOA, the characteristic absorption peaks of N-C and -OH can be detected at 1030 and 3400 cm⁻¹, respectively [22]. DDP showed P-O, C=O, and -OH peaks at 920, 1710, and 3400 cm⁻¹, respectively [23]. After esterification of TEOA and DDP, the resulting HPN showed not only the characteristic peaks of P-O, N-C, and C=O at 920, 1030, and 1710 cm⁻¹, but also a significant characteristic peak of the ester group at 1200 cm⁻¹, indicating that HPN was successfully synthesized. It was also noted that the mole ratio of -OH (in TEOA) and -COOH (in DDP) was 1.3: 1, so there were lots of hydroxyl groups in HPN, which could promote the transesterification of the vitrimer under heating.

The ¹H NMR of DDP and HPN are illustrated in Fig. 1c. Evidently, the proton shift of -COOH at 12.5 ppm in the ¹H NMR of DDP cannot be detected in that of HPN. In contrast, the chemical shift at 5.5 ppm in ¹H NMR of HPN was ascribed to -OH, suggesting that the carboxyl group in DDP was completely reacted by the excess -OH in TEOA. In addition, the chemical shift of the biphenyl group in DDP shifted from 7.0–8.5 ppm to 6.0–8.0 ppm after the esterification. In the ¹H NMR of HPN, the signal of aliphatic hydrocarbons from the DDP part appeared at 2.0–3.8 ppm, and those from the TEOA part arose at 2.8–5.0 ppm. As shown in Fig. 1d, HPN was similar to DDP, with a single chemical shift at 31.2 ppm in its ³¹P NMR, indicating that HPN was successfully synthesized. GPC results

displayed that HPN had a relative number average molecular weight of 3175 and its polydispersity was 1.9 (see Fig. S1), demonstrating that HPN was a hyperbranched polyester oligomer and its molecular weight distribution was relatively homogeneous. All these manifested the triumphant synthesis of a hyperbranched oligomer HPN by the esterification reaction between TEOA and DDP. HPN can covalently link to the crosslinking network as it contained lots of tertiary amine and hydroxyl groups, and these groups can catalyse the transesterification within the network at elevated temperatures. Thus, HPN_x was a well-designed self-catalytic epoxy vitrimer (see Fig. 1e).

3.2. Optical and mechanical properties

The high transparency of materials is a prerequisite for their applications in optical devices, transportation, construction, and other fields [24–26]. Consequently, the development of transparent vitrimers will significantly enhance their potential for industrial application and make a substantial contribution to the progress of industrialization in relevant fields. The UV-visible spectra of the vitrimers are presented in Fig. 2a. It is evident that the transmittance of the vitrimers within the wavelength of 200–330 nm was nearly 0. However, EP had a higher transmittance (~20%) in the wavelength of 300–330 nm. It indicated that all vitrimers possessed more excellent UV-shielding capabilities than EP. Subsequently, the transmittance of all specimens showed a progressive upward trend with increasing wavelength (from 400 to 900 nm). Furthermore, at an identical wavelength, the transmittance of the vitrimers diminished progressively with the augmentation of phosphorus content, but they remained proximate to EP. Specifically, the transmittance at the wavelength of 700 nm was 85.9% and 90.3% for HPN_{1.80} and EP, respectively (see Fig. S2). In addition, the image under the

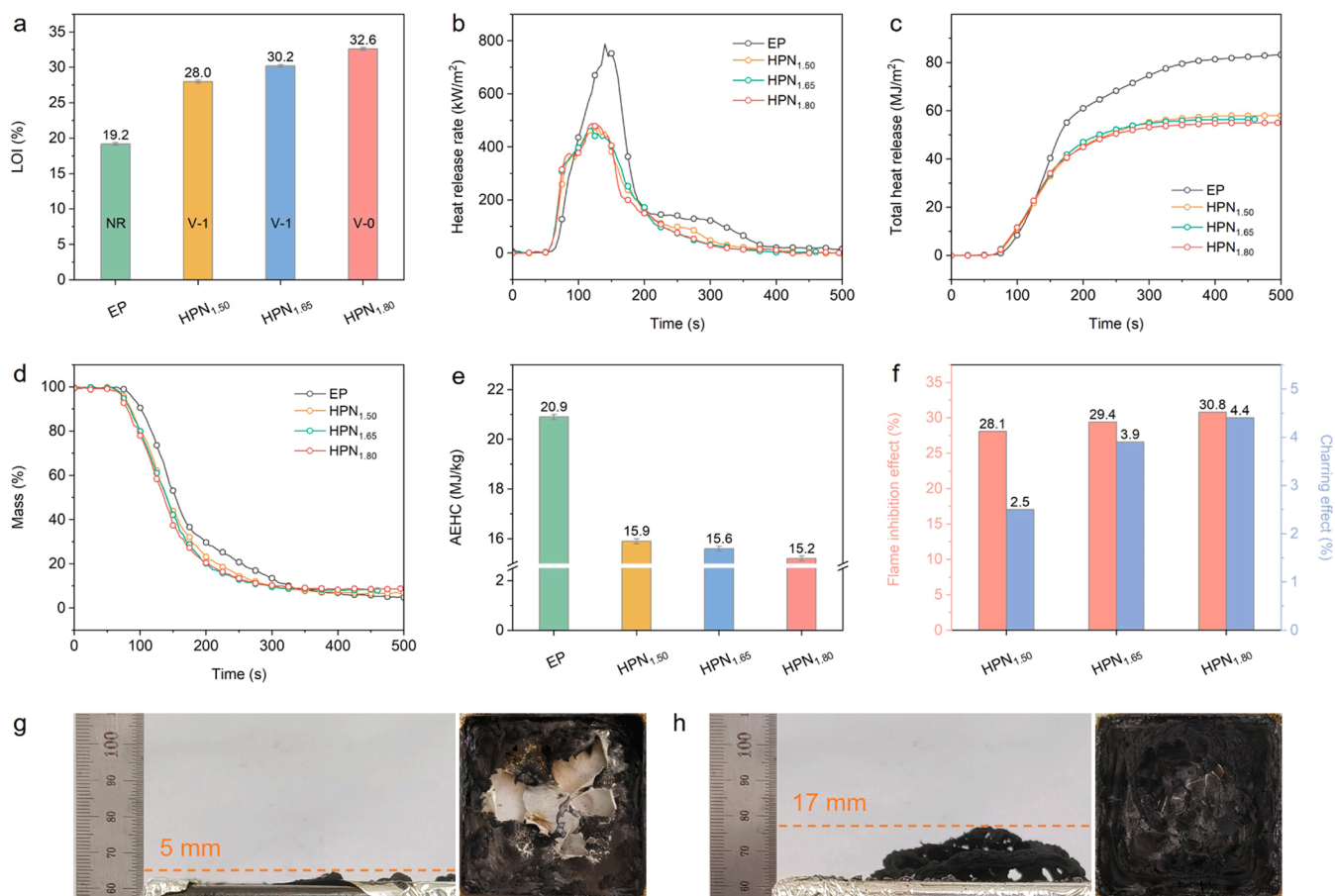


Fig. 4. (a) LOI and UL-94 results; (b) heat release rate curves; (c) total heat release plots; (d) mass loss curves; (e) AEHC of EP and HPN_x; (f) flame inhibition effect and charring effect of HPN_x; and digital images of (g) EP and (h) HPN_{1.80} chars after cone calorimetry tests.

vitriimer film can be easily observed (see Figs. 2a and S3). Thus, the resulting vitrimers have a high degree of transparency. The transparency of polymer is associated with its crystalline characteristics [27,28]. EP and HPN_x exhibited a wide diffraction peak centered at approximately $2\theta = 18^\circ$ (see Fig. 2b). Consequently, the hyperbranched polyester HPN did not have a substantial impact on the amorphous characteristics of DGEBA/MeTHPA, thereby the vitrimers can retain high transparency. The high transparency also verified that HPN was evenly dispersed in the cross-linked network, which was the basis for the other properties.

The dynamic mechanical properties of all specimens were examined through dynamic mechanical analysis (DMA). The crosslink density (ρ) was ascertained based on the classical theory of rubber [29,30], and the corresponding test results are presented in Fig. S4 and Table S2. The incorporation of HPN led to a significantly enhanced storage modulus (E') (at 30 °C) of HPN_x in comparison with that of EP (see Table S2), which was consistent with the variation in tensile modulus shown in Fig. 2c, indicating that the introduction of HPN improved the rigidity of epoxy vitrimers. The glass transition temperature (T_g) of the vitrimers decreased gradually with the addition of HPN, which was related to the decrease in ρ . Furthermore, the mechanical properties of EP and HPN_x were examined comprehensively (see Fig. 2c-f). As shown in Fig. 2c-f, HPN_x had significantly better mechanical properties than EP, which gradually improved as the loading level of HPN increased. HPN_{1.80} shows the best mechanical properties among all samples, and its tensile strength (σ), elongation at break (δ), toughness, impact strength (α_k), critical stress intensity factor (K_{IC}) and critical energy release rate (G_{IC}) reached 74.5 MPa, 5.9%, 2.3 MJ/m³, 4.5 kJ/m², 1.3 MPa·m^{1/2} and 5.4 kJ/m², which were 28.5%, 11.3%, 43.8%, 104.5%, 18.2% and 12.5% higher than those of EP, respectively. Hence, the hyperbranched

polyester HPN had a promising toughening and strengthening effect toward epoxy thermoset, and the toughening and strengthening effect of HPN was primarily attributed to the abundance of hydroxyl groups in its structure and its strong covalent interaction with the EP matrix.

The morphology of the fracture surface for EP and HPN_{1.80} specimens was analyzed by scanning electron microscopy (SEM) to investigate the toughening and strengthening mode-of-action for HPN. Their cross-sectional micrographs after Izod impact tests are depicted in Fig. 2g-h. EP exhibited smooth fracture surfaces, which indicated its brittle fracture behavior. In contrast, the cross-section of HPN_{1.80} was coarse due to the existence of HPN. Moreover, a large number of shear bands can be observed within the fractured surface of HPN_{1.80}. Additionally, both nitrogen and phosphorus atoms were uniformly distributed in the fractured surface of HPN_{1.80} (see Fig. 2h), which aligned with the optical results and further validated a favorable compatibility between EP and HPN. The covalent interaction of HPN with the matrix inhibited further crack propagation and dissipated numerous energies when the matrix was exposed to external forces [31–33]. To sum up, the hyperbranched polyester HPN successfully enhanced the toughness and strength of EP by regulating the cross-link density and forming a covalent interaction with the EP matrix.

3.3. Thermal performances

Thermogravimetric analysis (TGA) of EP and HPN_x was carried out in N₂ and air, and the characteristic results are presented in Fig. 3 and Table S3. The temperature at 5% weight loss ($T_{5\%}$) of HPN_x was lower than that of EP in both N₂ and air, which was related to the catalytic degradation of phosphorus-containing groups towards the matrix [34,

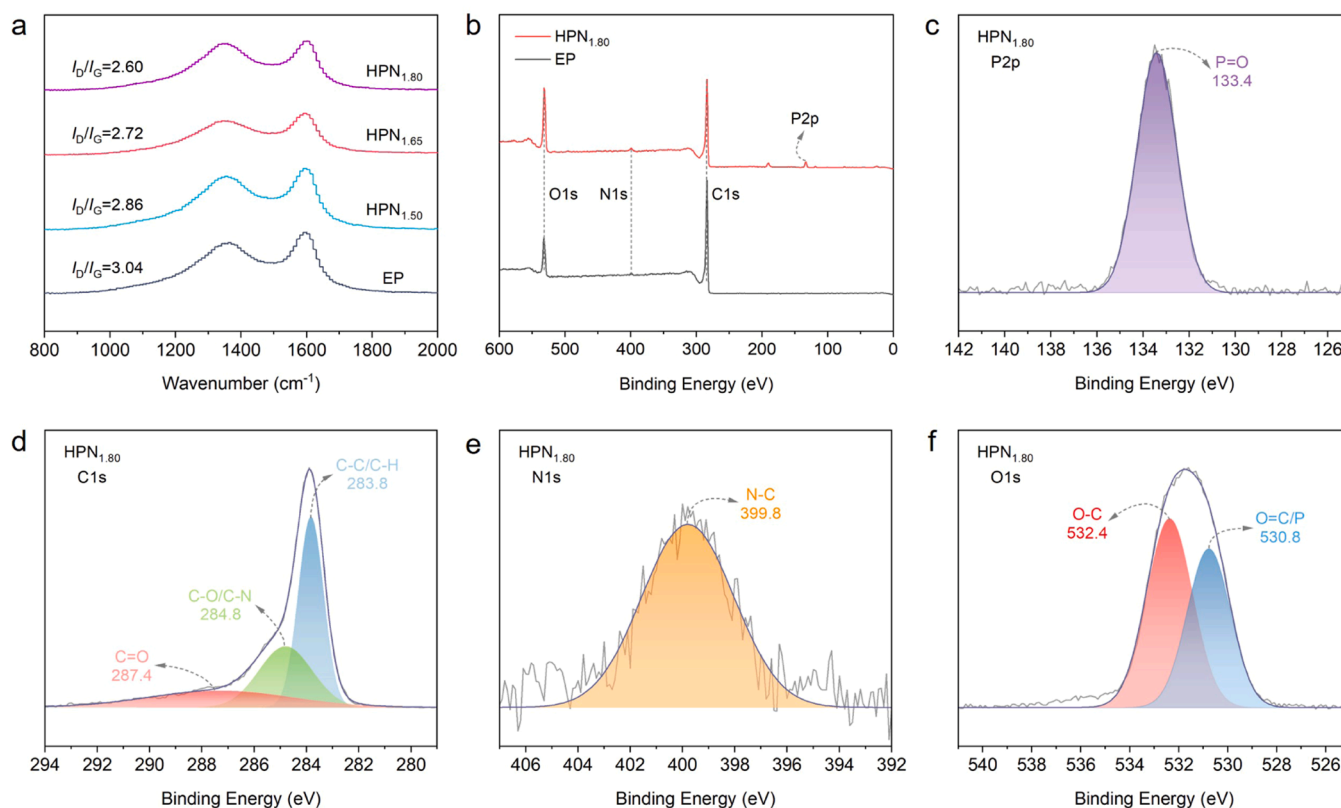


Fig. 5. (a) Raman spectra of residual chars for EP and HPN_x; (b) XPS full-scan spectra of residual chars for EP and HPN_{1.80}; high-resolution XPS (c) P2p, (d) C1s, (e) N1s, and (f) O1s spectra of residual char for HPN_{1.80}.

35]. In addition, the maximum weight loss rate (R_{max}) of HPN_x was lower than that of EP in both nitrogen and air, suggesting that HPN was able to suppress the matrix degradation at high temperatures. The char yield at 800 °C (CY) of HPN_x was significantly higher than that of EP in nitrogen, indicating that the introduction of HPN was beneficial to promoting residual char formation. As illustrated in Fig. 3b and d, the thermal decomposition of the matrix in air was divided into two stages. The first stage was associated with the fragmentation of the crosslinking network and the formation of chars, and the second stage was the thermal oxidative decomposition of the char formed in the first stage [33]. The temperature at maximum weight loss rate (T_{max}) was associated with these two stages. Evidently, with the addition of HPN, the T_{max2} of HPN_x increased progressively. It implied that the residual char generated by HPN_x at elevated temperatures had enhanced thermal stability, which might be associated with the existence of phosphorus-containing groups [36,37]. Overall, the addition of HPN was capable of effectively facilitating the generation of residual char and considerably augmenting its thermal stability.

3.4. Flame-retardant performances and modes-of-action

Due to the high content of H, C, and O in polymers, they frequently possess intrinsic flammability [38–40]. The fire safety is of paramount importance for polymers [41]. First, LOI and UL-94 tests were carried out on EP and HPN_x, and the relevant data are shown in Fig. 4a. The EP exhibited high flammability, as demonstrated by a relatively low LOI value of 19.2%, and it failed the UL-94 test. With the addition of HPN, the LOI and UL-94 ratings were remarkably enhanced. Specifically, the HPN_{1.50} attained a LOI of 28.0% and a UL-94 V-1 rating. When the phosphorus content was further increased to 1.80 wt%, the HPN_{1.80} passed a UL-94 V-0 rating with a high LOI of 32.6%. It also indicated that HPN_{1.80} was a self-extinguishing material.

To investigate the combustion behaviors of EP and HPN_x, the cone

calorimetry test (CCT) was performed, and the results are depicted in Fig. 4b–e and Table S4. Initially, the time to ignition (TTI) of HPN_x samples was shorter than that of EP (see Table S4) due to the pyrolysis of phosphorus-containing groups at relatively low temperatures, which was in line with the TGA results [42,43]. With the addition of HPN, the heat release of HPN_x was significantly reduced. Specifically, the peak heat release rate (PHRR) and total heat release (THR) of HPN_{1.80} reduced to 488.3 kW/m² and 55.0 MJ/m², with 38.0% and 33.9% decrease relative to those of EP. The average effective heat of combustion (AEHC) is employed to assess the combustion intensity of gas-phase volatiles [44,45]. The AEHC of HPN_{1.80} decreased from 20.9 MJ/kg of EP to 15.2 MJ/kg, representing a 27.3% reduction (see Fig. 4e). Apparently, the radical-quenching effect of P-containing decomposition fragments derived from HPN accounted for the diminished gas-phase combustion of the matrix. Moreover, the HPN_x vitrimer exhibited a substantially enhanced residual weight at flameout (RWF) compared to EP (see Table S4). The RWF of HPN_{1.80} raised from 4.6% of EP to 8.8%, with a 91.3% increment. Thus, HPN promoted the charring of the EP matrix during combustion, and such promoting effect can also be confirmed by the digital images of char residues in Fig. 4g and h. At the same time, the denseness and expansion degree of the HPN_{1.80} char were considerably improved relative to those of the EP char (see Fig. 4g and h). In terms of char thickness, the HPN_{1.80} showed a residual char thickness of 17 mm, with an improvement of 240% relative to EP char thickness (5 mm). Based on the work of Scharrel *et al.*, the flame inhibition effect (FIE) and charring effect (CE) are positively correlated with gaseous- and condensed-phase flame retardancy, respectively [46]. With the addition of HPN, the FIE and CE of HPN_x were gradually increased. The FIE for HPN_{1.80} increased to 30.8%, and the CE for HPN_{1.80} reached 4.4%. In conclusion, HPN functioned in both gas and condensed phases by means of flame inhibition and barrier/protective modes-of-action to restrain combustion, thereby improving flame retardancy.

The condensed-phase flame-retardant mode-of-action was first

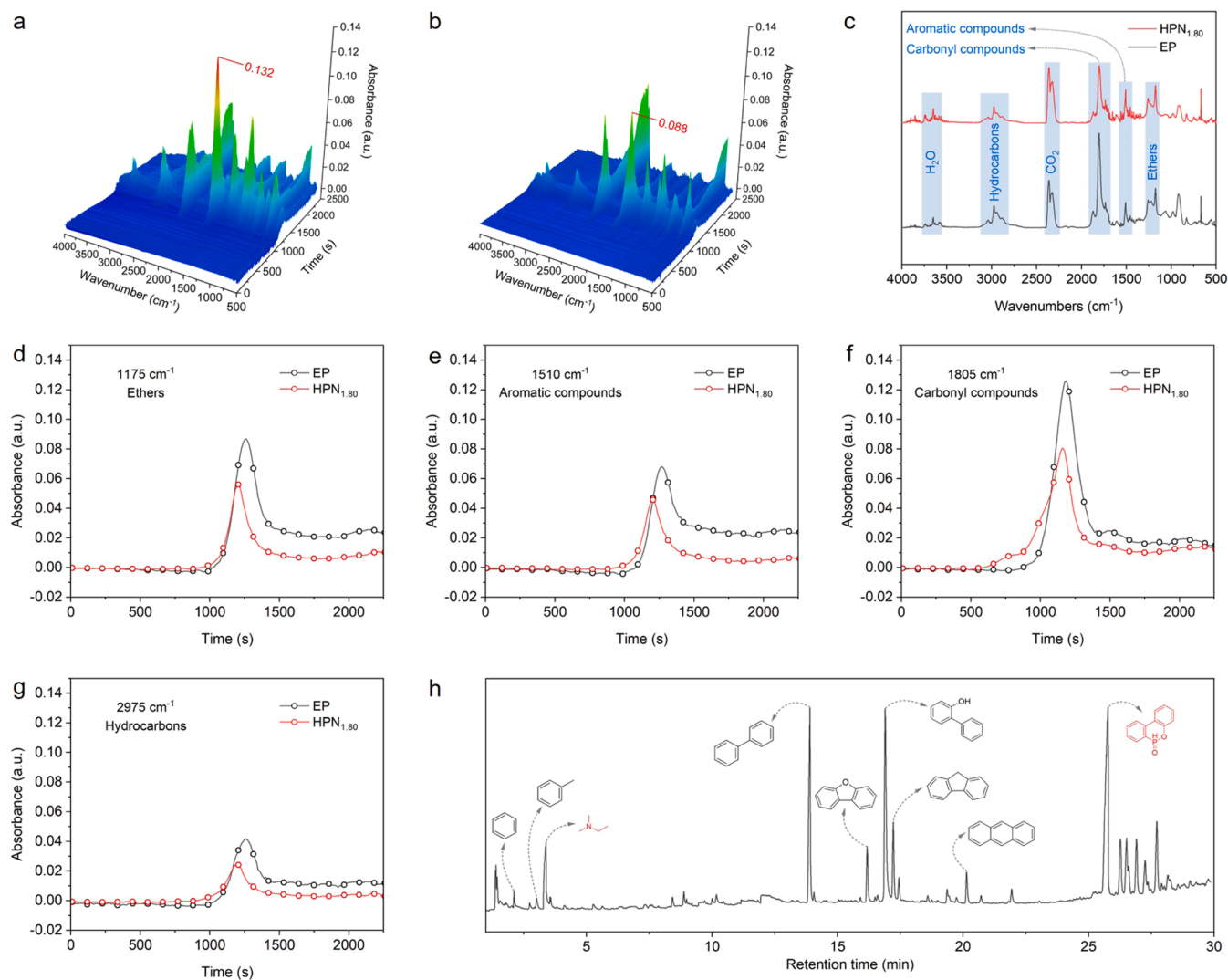


Fig. 6. 3D FTIR spectra of decomposition products for (a) EP and (b) HPN_{1.80}; (c) FTIR spectra of decomposition products for EP and HPN_{1.80} at T_{max} ; absorption vs. time curves of the characteristic peaks at (d) 1175, (e) 1510, (f) 1805, and (g) 2975 cm^{-1} for EP and HPN_{1.80}; and (h) total ion chromatogram of HPN.

verified by Raman spectroscopy. The D and G bands at 1360 and 1605 cm^{-1} can be found in the Raman spectra of residual chars, corresponding to the amorphous carbon and graphite structures, respectively (see Fig. 5a). The integrated area ratio of the D band to G band (I_D/I_G) is negatively correlated with the degree of graphitization of char. As the phosphorus content increased, the I_D/I_G value of residual chars decreased in a monotonous way, which suggested a higher degree of graphitization. Therefore, the decomposition products of HPN accelerated the charring of the vitrimers and enhanced the degree of graphitization for residual chars during burning. This in turn suppressed the heat release and oxygen transfer, leading to enhanced flame retardancy.

X-ray photoelectron spectroscopy (XPS) test was performed to analyze the chemical composition and bonding state of the vitrimer char obtained from CCT, with the spectra presented in Figs. 5 and S5. Three deconvolution peaks corresponding to C=O, C-O/C-N, and C-C/C-H were identified in the C1s spectra of HPN_{1.80} and EP chars (see Figs. 5d and S5a). The N-C peak appeared in the N1s spectra (see Figs. 5e and S5b). In the O1s spectrum of HPN_{1.80} char, two deconvolution peaks which were attributed to O-C and O=C/P can be observed (see Fig. 5f) [47]. The O content of HPN_{1.80} char rose from 19.39 wt% of EP char to 29.11 wt% (see Table S5). This indicated that the decomposition products of P-containing groups in HPN had interacted with the oxygen atom from the matrix during burning, thereby resulting in an augmented O

content. In addition, the P=O peak can be easily observed at 133.4 eV in the XPS P2p spectrum of HPN_{1.80} char (see Fig. 5c). Furthermore, the HPN_{1.80} contained up to 7.03 wt% of phosphorus (see Table S5). Thus, HPN pyrolyzed into phosphate derivatives during combustion, which promoted the formation of a more stable char layer on the matrix surface to inhibit heat-oxygen exchange and enhance flame retardancy.

The gas-phase mode-of-action was probed by thermogravimetric analysis-infrared spectrometry (TG-IR) and pyrolysis-gas chromatography/mass spectrometry (Py-GC/MS) tests. Firstly, the incorporation of HPN led to a significant reduction in the R_{max} (see Figs. 6a and 6b). The decomposition products of EP and HPN_{1.80} were similar, and they primarily consisted of ethers (1175 cm^{-1}), aromatic compounds (1510 cm^{-1}), carbonyl compounds (1805 cm^{-1}), carbon dioxide (2365 cm^{-1}), hydrocarbons (2975 cm^{-1}), and water (3650 cm^{-1}) (see Fig. 6c) [48,49]. Notably, the absorption intensities of the majority of HPN_{1.80} fragments were inferior to those of EP (see Fig. 6d-g). Therefore, during combustion, the decomposition products of HPN significantly inhibited the thermal decomposition of the matrix and promoted the charring. In addition, the total ion chromatogram and the main pyrolysis products of HPN are summarised in Fig. 6h and Table S6. The main pyrolysis products of HPN were aromatic derivatives, nitrogen-containing derivatives, and phosphorus-containing fragments. There were lots of aromatic compounds released at the retention time of

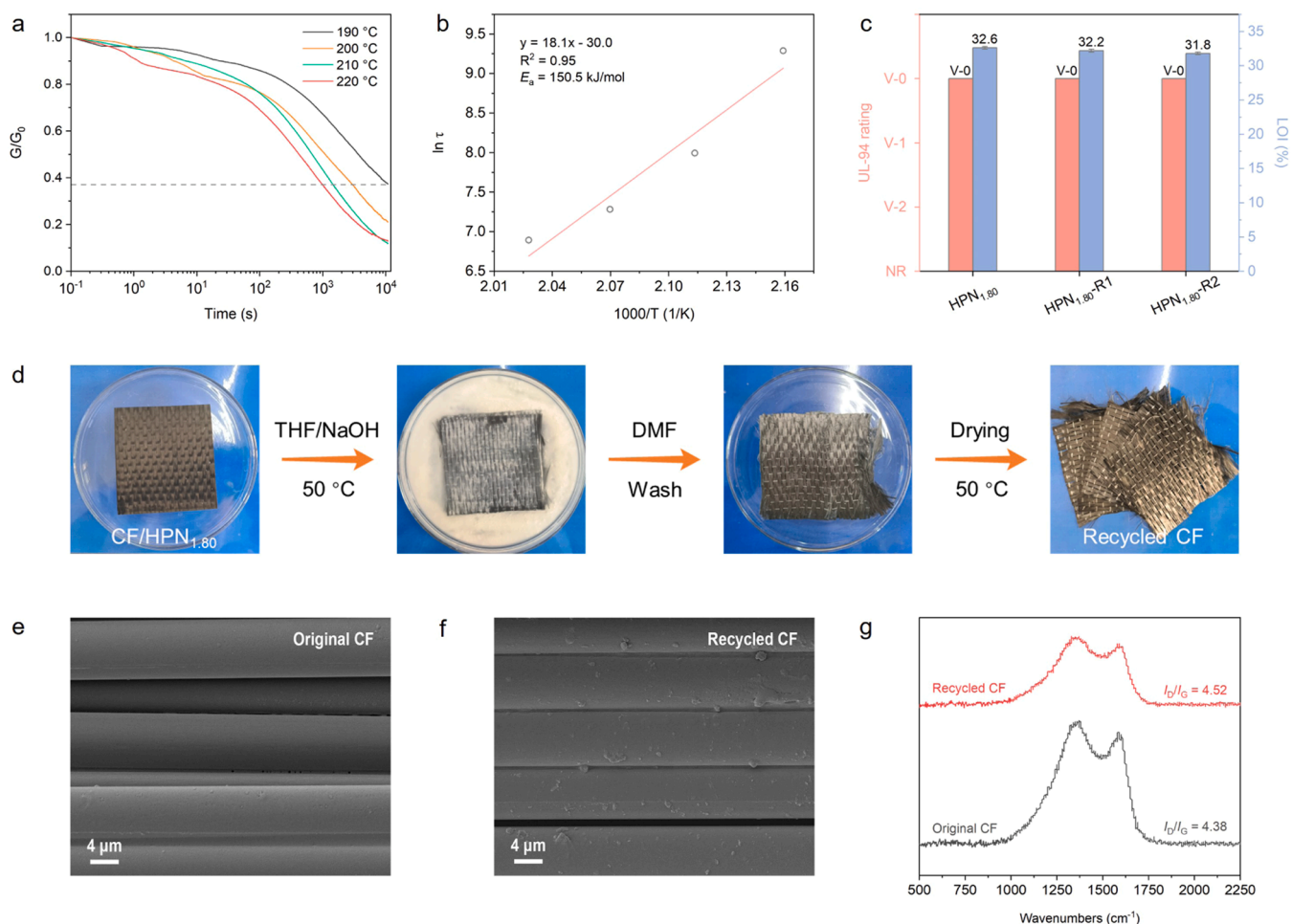


Fig. 7. (a) Normalized stress relaxation curves of HPN_{1.80} at different temperatures; (b) linear fitting to the Arrhenius equation; (c) UL-94 and LOI results of HPN_{1.80} and recycled HPN_{1.80} (by hot-pressing at 200 °C for 1 h); (d) illustration of the recycling process for CF/HPN_{1.80} composite (composites surface area: approx. 8 cm × 8 cm); SEM of (e) original and (f) recycled CFs; and (g) Raman spectra of original and recycled CFs.

2.1, 3.0, 13.9, 16.2, 17.2, and 20.1 min, which was related to the high content of aromatic compounds in HPN. Moreover, at the retention time of 3.25 min, HPN released some nitrogen-containing derivatives which can dilute the concentration of combustible gases during combustion and inhibit the combustion reaction. At the retention time of 25.8 min, HPN releases numerous phosphorus-containing fragments which can be further decomposed into P-containing radicals to inhibit gas-phase combustion by quenching active radicals generated by the EP matrix. In summary, HPN retarded the gas-phase combustion reaction by releasing phosphorus-containing radicals and inert gases during combustion. Consequently, the excellent flame retardancy of HPN_x vitrimers was attributed to the bi-phase modes of action for HPN.

3.5. Physical and chemical recovery

Dynamic exchange reactions in vitrimer are commonly studied *via* stress relaxation measurements [50,51]. The stress relaxation curves of HPN_{1.80} at different temperatures are shown in Fig. 7a. The relaxation time (τ^*) represents the time needed for the stress to decline to 1/e of its initial value. As shown in Fig. 7a, the relaxation time shortened as the temperature increased, suggesting that higher temperature facilitated transesterification. The activation energy (E_a) was calculated by fitting the τ^* of HPN_{1.80} to the Arrhenius equation: $\ln \tau^* = E_a/RT - \ln A$ [52, 53]. The obtained linear fit curve presented an activation energy of 150.5 kJ/mol (see Fig. 7b). It showed that HPN_{1.80} had favorable stability at high temperatures. To further confirm the recyclability of

HPN_{1.80}, we recovered the sheared HPN_{1.80} by hot pressing at 200 °C for 1 h, and the resulting sample was noted as HPN_{1.80}-R_y, where y represented the recovery times. The LOI and UL-94 results of HPN_{1.80} and HPN_{1.80}-R_y are compared in Fig. 7c, and the LOI of HPN_{1.80}-R2 was 97.5% of that of HPN_{1.80}, and it still achieved a UL-94 V-0 rating. Therefore, it can be concluded that HPN_{1.80} vitrimer can be reused sustainably as flame retardant material.

Fabricating CFRP composites constitutes a crucial utilization of thermoset resins [54,55]. However, it is challenging to recycle CF from carbon fiber-reinforced thermoset composites. The dilemma can be solved with vitrimer. The fracture of the ester group can be carried out under alkaline conditions. Thus, CFs can be chemically recovered from CF/HPN_{1.80} composites. The well-prepared CF/HPN_{1.80} composite was immersed in THF/NaOH solution (8: 2, v/v) at 50 °C for 3 d, and the vitrimer was dissolved in the solution (see Fig. 7d). The recovered CFs were cleaned by DMF and dried in an oven. The surface morphology and I_D/I_G of the recovered CFs were examined, and the outcomes are presented in Fig. 7e-g. The recovered CFs showed a clean surface, which was close to that of the original CFs, suggesting that the HPN_{1.80} was entirely detached from the CFs. Moreover, the I_D/I_G of the recycled CFs was 4.52, which was close to 4.38 of the original CFs (see Fig. 7g). The recovered CFs showed a similar degree of graphitization as before recovery, indicating that the CFs were recovered in a non-destructive manner. Thus, the HPN_{1.80} vitrimer holds significant potential for utilization in the fabrication of high-tech recyclable CFRP composites.

4. Conclusions

In this study, a transparent, toughened, and flame-retardant HPN_{1.80} vitrimer was developed based on a rationally designed phosphorus/tertiary amine/polyhydroxy hyperbranched polyester (HPN). HPN_{1.80} had favorable transparency and toughness due to the good compatibility and covalent interaction between HPN and the matrix. The HPN_{1.80} vitrimer featured self-extinguishing properties (LOI: 32.6% and UL-94 V-0) due to the flame-retardant effect of phosphorus and nitrogen in the gas/condensed phases. Importantly, HPN_{1.80} can be remodeled due to the co-catalysis of the tertiary amine and hydroxyl groups, and its LOI and UL-94 rating remained essentially unchanged after two physical reprocessings. In addition, the CFs in the carbon fiber-reinforced HPN_{1.80} composites can be recovered without damage. In this study, we provide a simple and effective strategy for the preparation of closed-loop recyclable vitrimers with excellent transparency, toughness, and flame retardancy, which is expected to accelerate the practical application of vitrimers in the fields of construction, transportation, and electronics.

CRedit authorship contribution statement

Guo Yong: Formal analysis. **Wang Cheng:** Resources, Data curation. **Huo Siqi:** Writing – review & editing, Supervision, Funding acquisition, Conceptualization. **Ye Guofeng:** Writing – original draft, Investigation. **Liu Zhitian:** Supervision. **Wang Hao:** Supervision. **Song Pingan:** Supervision. **Yang Qingshan:** Data curation.

Declaration of Competing Interest

The authors declare that they have no known competing financial interests or personal relationships that could have appeared to influence the work reported in this paper.

Acknowledgments

This work was funded by the Australian Research Council (DE230100616 and DP240102628).

Appendix A. Supporting information

Supplementary data associated with this article can be found in the online version at [doi:10.1016/j.conbuildmat.2025.140673](https://doi.org/10.1016/j.conbuildmat.2025.140673).

Data Availability

Data will be made available on request.

References

- Y. Jiang, J. Li, D. Li, Y. Ma, S. Zhou, Y. Wang, D. Zhang, Bio-based hyperbranched epoxy resins: synthesis and recycling, *Chem. Soc. Rev.* 53 (2) (2024) 624–655.
- S. Huo, P. Song, B. Yu, S. Ran, V.S. Chevali, L. Liu, Z. Fang, H. Wang, Phosphorus-containing flame retardant epoxy thermosets: recent advances and future perspectives, *Prog. Polym. Sci.* 114 (2021) 101366.
- J. Luo, Z. Demchuk, X. Zhao, T. Saito, M. Tian, A.P. Sokolov, P.-F. Cao, Elastic vitrimers: beyond thermoplastic and thermoset elastomers, *Matter* 5 (5) (2022) 1391–1422.
- Y. Yang, Y. Xu, Y. Ji, Y. Wei, Functional epoxy vitrimers and composites, *Prog. Mater. Sci.* 120 (2021) 100710.
- P. Yu, H. Wang, T. Li, G. Wang, Z. Jia, X. Dong, Y. Xu, Q. Ma, D. Zhang, H. Ding, B. Yu, Mechanically robust, recyclable, and self-healing polyimine networks, *Adv. Sci.* 10 (19) (2023) e2300958.
- Y. Zhang, H. Yan, R. Yu, J. Yuan, K. Yang, R. Liu, Y. He, W. Feng, W. Tian, Hyperbranched dynamic crosslinking networks enable degradable, reconfigurable, and multifunctional epoxy vitrimer, *Adv. Sci.* 11 (2) (2024) e2306350.
- C.A. Tretbar, J.A. Neal, Z. Guan, Direct silyl ether metathesis for vitrimers with exceptional thermal stability, *J. Am. Chem. Soc.* 141 (42) (2019) 16595–16599.
- G.M. Scheutz, J.J. Lessard, M.B. Sims, B.S. Sumerlin, Adaptable crosslinks in polymeric materials: resolving the intersection of thermoplastics and thermosets, *J. Am. Chem. Soc.* 141 (41) (2019) 16181–16196.
- J. Zheng, Z.M. Png, S.H. Ng, G.X. Tham, E. Ye, S.S. Goh, X.J. Loh, Z. Li, Vitrimers: current research trends and their emerging applications, *Mater. Today* 51 (2021) 586–625.
- D. Montarnal, M. Capelot, F. Tournilhac, L. Leibler, Silica-like malleable materials from permanent organic networks, *Science* 334 (2011) 965–968.
- J.J.B. van der Tol, S. Hafeez, A.P.G. Bänziger, H. Su, J.P.A. Heuts, E.W. Meijer, G. Vantomme, Supramolecular polymer additives as repairable reinforcements for dynamic covalent networks, *Adv. Mater.* 36 (49) (2024) 2410723.
- Y. Xu, H. Zhang, S. Dai, S. Xu, J. Wang, L. Bi, J. Jiang, Y. Chen, Hyperbranched polyester catalyzed self-healing bio-based vitrimer for closed-loop recyclable carbon fiber-reinforced polymers, *Compos. Sci. Technol.* 228 (2022) 109676.
- F.I. Altuna, C.E. Hoppe, R.J.J. Williams, Epoxy vitrimers with a covalently bonded tertiary amine as catalyst of the transesterification reaction, *Eur. Polym. J.* 113 (2019) 297–304.
- D. Berne, F. Cuminet, S. Lemouzy, C. Joly-Duhamel, R. Poli, S. Caillol, E. Leclerc, V. Ladmiral, Catalyst-free epoxy vitrimers based on transesterification internally activated by an α -CF₃ group, *Macromolecules* 55 (5) (2022) 1669–1679.
- L. Yue, K. Ke, M. Amirhosravi, T.G. Gray, I. Manas-Zloczower, Catalyst-free mechanochemical recycling of bio-based epoxy with cellulose nanocrystals, *ACS Appl. Bio Mater.* 4 (5) (2021) 4176–4183.
- X.-Q. Chen, Y.-C. Lin, W.-B. Bai, Y.-W. Yan, R.-K. Jian, Nonconventional phosphorus-based tertiary amine curing agent enabling the high fire safety, outstanding tensile strength and high glass transition temperature of epoxy resin, *Chem. Eng. J.* 505 (2025) 159293.
- K.-X. Liang, J.-L. Chen, Y.-C. Lin, W.-B. Bai, R.-K. Jian, Natural resin-derived urushiol-based phosphorylation derivative towards flame-retardant and mechanically strong epoxy resin, *Polym. Degrad. Stab.* 229 (2024) 110985.
- K.R. Ren, S. Gu, Y.Z. Wang, L. Chen, A phosphonate-derived epoxy vitrimer with intrinsic flame retardancy and catalyst-free reprocessability, *J. Polym. Sci.* 62 (14) (2023) 3195–3205.
- G. Ye, S. Huo, C. Wang, Q. Shi, L. Yu, Z. Liu, Z. Fang, H. Wang, A novel hyperbranched phosphorus-boron polymer for transparent, flame-retardant, smoke-suppressive, robust yet tough epoxy resins, *Compos. Part B: Eng.* 227 (2021) 109395.
- Q. Shi, S. Huo, C. Wang, G. Ye, L. Yu, Z. Fang, H. Wang, Z. Liu, A phosphorus/silicon-based, hyperbranched polymer for high-performance, fire-safe, transparent epoxy resins, *Polym. Degrad. Stab.* 203 (2022) 110065.
- G. Ye, S. Huo, C. Wang, P. Song, Z. Fang, H. Wang, Z. Liu, Durable flame-retardant, strong and tough epoxy resins with well-preserved thermal and optical properties via introducing a bio-based, phosphorus-phosphorus, hyperbranched oligomer, *Polym. Degrad. Stab.* 207 (2023) 110235.
- F. Luo, S. Yang, X. Yang, Y. Feng, B. Lin, Y. Zou, H. Li, Catalyst-free sustainable epoxy vitrimers with fire safety offered by phosphorus-containing compounds, *Polym. Degrad. Stab.* 230 (2024) 111042.
- H. Zhao, H. Duan, J. Zhang, L. Chen, C. Wan, C. Zhang, C. Liu, H. Ma, An Itaconic acid-based phosphorus-containing oligomer endowing epoxy resins with good flame retardancy and toughness, *Macromol. Mater. Eng.* 308 (4) (2022) 2200550.
- Q. Zhong, B. Gao, Y. Weng, S. Zhang, Adopting intrinsic hydrophilic thermoplastic starch composites to fabricate antifogging sustainable films with high antibiosis and transparency, *ACS Sustain. Chem. Eng.* 10 (11) (2022) 3661–3672.
- Y. Zhang, R. Liu, R. Yu, K. Yang, L. Guo, H. Yan, Phosphorus-free hyperbranched polyborate flame retardant: ultra-high strength and toughness, reduced fire hazards and unexpected transparency for epoxy resin, *Compos. Part B: Eng.* 242 (2022) 110101.
- Y. Yuan, Q. Zhang, X. Luo, R. Gu, Experimental study on the mechanical properties of the reinforced transparent building membrane material STFE, *Constr. Build. Mater.* 409 (2023) 133849.
- C. Wang, S. Huo, G. Ye, P. Song, H. Wang, Z. Liu, A P/Si-containing polyethylenimine curing agent towards transparent, durable fire-safe, mechanically-robust and tough epoxy resins, *Chem. Eng. J.* 451 (2023) 138768.
- G. Ye, S. Huo, C. Wang, Q. Zhang, H. Wang, P. Song, Z. Liu, Strong yet tough catalyst-free transesterification vitrimer with excellent fire-retardancy, durability, and closed-loop recyclability, *Small* 20 (45) (2024) 2404634.
- Y. Wang, R. Shu, X. Zhang, Strong, SUPertough and Self-healing Biomimetic Layered Nanocomposites Enabled by Reversible Interfacial Polymer Chain Sliding, *Angew. Chem. Int. Ed.* 62 (23) (2023) e202303446.
- M.A.A. Ahmad, M.S. Abdul Majid, M.J.M. Ridzuan, M.N. Mazlee, A.G. Gibson, Dynamic mechanical analysis and effects of moisture on mechanical properties of interwoven hemp/polyethylene terephthalate (PET) hybrid composites, *Constr. Build. Mater.* 179 (2018) 265–276.
- G. Lou, Z. Ma, J. Dai, Z. Bai, S. Fu, S. Huo, L. Qian, P. Song, Fully biobased surface-functionalized microcrystalline cellulose via green self-assembly toward fire-retardant, strong, and tough epoxy biocomposites, *ACS Sustain. Chem. Eng.* 9 (40) (2021) 13595–13605.
- J. Wang, J. Wang, S. Yang, X. Chen, K. Chen, G. Zhou, X. Liu, L. Xu, S. Huo, P. Song, H. Wang, Multifunctional phosphorus-containing imidazoliums endowing one-component epoxy resins with superior thermal latency, heat resistance, mechanical properties, and fire safety, *Chem. Eng. J.* 485 (2024) 149852.
- J. Zhang, X. Mi, S. Chen, Z. Xu, D. Zhang, M. Miao, J. Wang, A bio-based hyperbranched flame retardant for epoxy resins, *Chem. Eng. J.* 381 (2020) 122719.
- C. Wang, G. Ye, Q. Zhang, H. Wang, S. Huo, Z. Liu, Closed-loop recyclable, self-catalytic transesterification vitrimer coatings with superior adhesive strength, fire retardancy, and environmental stability, *ACS Mater. Lett.* 7 (1) (2024) 210–219.
- C. Wang, S. Huo, G. Ye, Q. Zhang, C.-F. Cao, M. Lynch, H. Wang, P. Song, Z. Liu, Strong self-healing close-loop recyclable vitrimers via complementary dynamic covalent/non-covalent bonding, *Chem. Eng. J.* 500 (2024) 157418.

- [36] T. Liu, J. Peng, J. Liu, X. Hao, C. Guo, R. Ou, Z. Liu, Q. Wang, Fully recyclable, flame-retardant and high-performance carbon fiber composites based on vanillin-terminated cyclophosphazene polyimine thermosets, *Compos. Part B: Eng.* 224 (2021) 109188.
- [37] Q. Zhang, J. Wang, S. Yang, J. Cheng, G. Ding, Y. Hu, S. Huo, Synthesis of a P/N/S-based flame retardant and its flame retardant effect on epoxy resin, *Fire Saf. J.* 113 (2020) 102994.
- [38] Y. Chen, H. Duan, S. Ji, H. Ma, Novel phosphorus/nitrogen/boron-containing carboxylic acid as co-curing agent for fire safety of epoxy resin with enhanced mechanical properties, *J. Hazard. Mater.* 402 (2021) 123769.
- [39] T. Sai, X. Ye, B. Wang, Z. Guo, J. Li, Z. Fang, S. Huo, Transparent, intrinsically fire-safe yet impact-resistant poly(carbonates-*b*-siloxanes) containing Schiff-base and naphthalene-sulfonate, *J. Mater. Sci. Technol.* 225 (2025) 11–20.
- [40] X. Wang, E.N. Kalali, J.-T. Wan, D.-Y. Wang, Carbon-family materials for flame retardant polymeric materials, *Prog. Polym. Sci.* 69 (2017) 22–46.
- [41] X. Zhang, Z. Wang, S. Ding, Z. Wang, X. Xie, Improved thermal insulation, mechanical properties, energy absorption and flame retardancy of bio-based rigid polyurethane foam modified with calcium hydroxystannate, *Constr. Build. Mater.* 456 (2024) 139251.
- [42] S. Jin, L. Qian, Y. Qiu, Y. Chen, F. Xin, High-efficiency flame retardant behavior of bi-DOPO compound with hydroxyl group on epoxy resin, *Polym. Degrad. Stab.* 166 (2019) 344–352.
- [43] C. Liu, K. Huang, R. Liu, Y. Li, L. Dai, W. Wang, A multi-element flame retardant on the basis of silicon-phosphorus-nitrogen for combustibility suppressing of epoxy, *Polym. Test.* 111 (2022) 107582.
- [44] X. Zhou, S. Qiu, X. Mu, M. Zhou, W. Cai, L. Song, W. Xing, Y. Hu, Polyphosphazenes-based flame retardants: a review, *Compos. Part B: Eng.* 202 (2020) 108397.
- [45] S. Huo, S. Yang, J. Wang, J. Cheng, Q. Zhang, Y. Hu, G. Ding, Q. Zhang, P. Song, A liquid phosphorus-containing imidazole derivative as flame-retardant curing agent for epoxy resin with enhanced thermal latency, mechanical, and flame-retardant performances, *J. Hazard. Mater.* 386 (2020) 121984.
- [46] S. Brehme, B. Schartel, J. Goebbels, O. Fischer, D. Pospiech, Y. Bykov, M. Döring, Phosphorus polyester versus aluminium phosphinate in poly(butylene terephthalate) (PBT): Flame retardancy performance and mechanisms, *Polym. Degrad. Stab.* 96 (5) (2011) 875–884.
- [47] G. Ye, C. Wang, Q. Zhang, P. Song, H. Wang, S. Huo, Z. Liu, Bio-derived Schiff base vitrimer with outstanding flame retardancy, toughness, antibacterial, dielectric and recycling properties, *Int. J. Biol. Macromol.* 278 (2024) 134933.
- [48] P. Sun, H. Zhang, Y. Leng, Z. Wang, J. Zhang, M. Xu, X. Li, B. Li, Construction of flame retardant functionalized carbon dot with insulation, flame retardancy and thermal conductivity in epoxy resin, *Constr. Build. Mater.* 451 (2024) 138853.
- [49] J.-X. Yang, Y. Sun, W.-M. Song, Y. Liu, A novel phosphorus/boron-containing flame retardant for improving the flame retardancy of ramie fiber reinforced epoxy composites, *Constr. Build. Mater.* 451 (2024) 138814.
- [50] D.J. Fortman, J.P. Brutman, C.J. Cramer, M.A. Hillmyer, W.R. Dichtel, Mechanically activated, catalyst-free polyhydroxyurethane vitrimers, *J. Am. Chem. Soc.* 137 (44) (2015) 14019–14022.
- [51] F. Cuminet, S. Caillol, É. Dantras, É. Leclerc, V. Ladmiraal, Neighboring group participation and internal catalysis effects on exchangeable covalent bonds: application to the thriving field of vitrimer chemistry, *Macromolecules* 54 (9) (2021) 3927–3961.
- [52] J. Liu, K.V. Bernaerts, Preparation of lignin-based imine vitrimers and their potential application as repairable, self-cleaning, removable and degradable coatings, *J. Mater. Chem. A* 12 (5) (2024) 2959–2973.
- [53] L. Zhong, Y. Hao, J. Zhang, F. Wei, T. Li, M. Miao, D. Zhang, Closed-loop recyclable fully bio-based epoxy vitrimers from ferulic acid-derived hyperbranched epoxy resin, *Macromolecules* 55 (2) (2022) 595–607.
- [54] Y.-Y. Liu, G.-L. Liu, Y.-D. Li, Y. Weng, J.-B. Zeng, Biobased high-performance epoxy vitrimer with UV shielding for recyclable carbon fiber reinforced composites, *ACS Sustain. Chem. Eng.* 9 (12) (2021) 4638–4647.
- [55] J.-H. Chen, B.-W. Liu, J.-H. Lu, P. Lu, Y.-L. Tang, L. Chen, Y.-Z. Wang, Catalyst-free dynamic transesterification towards a high-performance and fire-safe epoxy vitrimer and its carbon fiber composite, *Green. Chem.* 24 (18) (2022) 6980–6988.